Take, W. A. & Bolton, M. D. (2011). *Géotechnique* **61**, No. 9, 757–769 [**doi:** 10.1680/geot.9.P.125]

Seasonal ratcheting and softening in clay slopes, leading to first-time failure

W. A. TAKE* and M. D. BOLTON†

Centrifuge tests have been carried out on kaolin clay slopes subject to variations in surface rainfall and humidity corresponding, at model scale, to successive wet and dry seasons in the field. These model slopes have been instrumented with miniature high-capacity tensiometers, and the deformations of their cross-sections have been observed by digital photography and analysed by particle image velocimetry. Sequences of swelling and shrinkage have been seen to be potentially irreversible, leading to creep in the form of down-slope ratcheting, accompanied by progressive regional softening within the zone affected by the seasonal moisture movements. Ultimately, this regional softening has been seen to lead to slope failures, in which segments of soil have separated from the mass through the opening of tension cracks and the formation of a localised shear rupture. An analysis of the phase of episodic regional softening is presented here, based on a Spencer limit-equilibrium approach. These back-analyses illustrate that clay slopes which temporarily mobilise an average stress ratio in excess of the critical state stress ratio during any portion of a typical year may eventually be brought to a long-term failure under the action of seasonal variations of pore pressure. Conversely, it is hypothesised that clay slopes which can maintain their overall equilibrium without exceeding the critical state stress ratio may not experience progressive seasonal softening.

KEYWORDS: centrifuge modelling; clays; failure; slopes

Des essais centrifuges ont été effectués sur des pentes d'argiles kaolinique soumises à des variations des niveaux de précipitation et d'humidité, correspondant, à l'échelle du modèle, à une succession de saisons humides et sèches sur le terrain. Les instruments installés sur ces pentes modèles étaient des tensiomètres miniature de capacité supérieure ; les déformations de leurs sections transversales ont été observées par photographie numérique, et analysés par PIV. Des séquences de gonflement puis de rétrécissement se sont avérées potentiellement irréversibles, et donnaient lieu à un fluage sous forme de rochetage suivant la ligne de la pente, accompagné d'un adoucissement régional progressif au sein de la zone affectée, sous l'effet des fluctuations saisonnières de l'humidité. En définitive, on a relevé que cet adoucissement régional engendrait des éboulements de pentes, dans le cadre desquels des segments de sol se séparaient de la masse à travers l'ouverture de fissures de contrainte et la formation d'une rupture par cisaillement localisée. On présente une analyse de la phase d'adoucissement régional épisodique, basée sur une méthode à équilibre limite de Spencer. Ces rétro-analyses illustrent le fait que des pentes d'argile mobilisant provisoirement un rapport de tensions moyen supérieur au rapport de tension d'état critique pendant une partie quelconque d'une année typique risquent d'être soumises à un éboulement à long terme sous l'action de variations saisonnières de la pression interstitielle. Inversement, on avance également l'hypothèse d'après laquelle des pentes d'argile en mesure de maintenir leur équilibre intégral sans dépasser le rapport de tension d'état critique pourront ne pas subir un adoucissement saisonnier progressif.

INTRODUCTION

Since the development of limit equilibrium methods to perform effective stress analyses of slope stability, questions have arisen regarding the appropriate choice of effective stress strength parameters which will maintain stability and limit deformations. In particular, the strength of a soil which can be safely mobilised to avoid first-time failure in a clay slope remains a topic of discussion in the literature. Researchers at Imperial College (e.g. Skempton, 1964; Bishop, 1967) were the first to emphasise the significance of progressive failure in the case of stiff clay slopes. Such soils exhibit brittle strain softening behaviour, with a peak undisturbed strength far above that given by the critical state friction angle (e.g. $\phi'_{cs} \approx 20^\circ$ for London Clay (Skempton, 1977)), and a residual strength significantly below the critical state friction angle after shear displacements sufficient to polish the slip surface (e.g. $c' = 1$ kPa, $\phi'_r = 13^\circ$ for London Clay (Skempton, 1977)). This very wide range of soil strength between peak and residual means that the decision on design soil strength will inevitably have significant implications for the cost and safety of proposed slope schemes.

Apart from the uncertainty in the effective strength envelope for design, clay slopes are subjected to a wide range of pore pressure conditions depending on the possible location of more permeable strata and their hydraulic conditions, and on the preceding weather. Here, a complicating factor is the likely existence of negative pore pressures induced in the short term by unloading due to slope cutting and in dry seasons by evapotranspiration, and the rate of swelling when water becomes available at the boundaries: see Vaughan and Walbancke (1973). Designers have the difficult task of selecting an appropriately high phreatic surface from which design pore pressures can be obtained. These must obviously exceed any values measured during ground investigation so as to encompass the wettest foreseeable conditions taking the weather, and transient flow, into account.

It is not surprising, therefore, that stiff clay slopes suffer slip failures, but fortunately these are rarely unheralded. In order to help clarify the changing behaviour of unstable

Manuscript received 20 July 2006; revised manuscript accepted 15 April 2010. Published online ahead of print 25 January 2011. Discussion on this paper closes on 1 February 2012, for further details see p. ii.

* Department of Civil Engineering, Queen's University, Kingston, Ontario, Canada.
† Director of the Schofield Centre, Cambridge University Engineering Department, Cambridge, UK.

slopes as failure progresses, Leroueil *et al.* (1996) and Leroueil (2001) have divided these slope instability processes into four stages of behaviour consisting of the pre-failure, first-time failure, post-failure and reactivation stages (Fig. 1). In the first stage, the slope has yet to experience first-time failure; this should apply to most engineered slopes, of course. These researchers state that slope behaviour in this pre-failure stage primarily consists of deformations arising from the combined influences of pore pressure changes, creep and progressive failure. If progressive failure is allowed to continue to a point where the slope can no longer maintain equilibrium, the second stage of first-time failure is reached. The third stage suggested by Leroueil (2001) is post-failure, and includes all soil displacements from the onset of failure until the soil mass comes to rest. The final stage of slope movement is the reactivation stage, in which the slope occasionally becomes active along its pre-existing rupture surfaces.

The residual friction angle is clearly the correct choice of strength parameter to avoid occasional reactivation of an unstable slope on an existing slip surface. However, the parameters to be chosen to avoid first-time failure are much less obvious. Initially, Skempton recommended in his Rankine Lecture (Skempton, 1964) that residual state strength parameters be chosen to avoid long-term first-time failures in London Clay, as this would completely preclude the possibility of failure. However, Skempton's later back analyses of slope failures in the London Clay (e.g. Skempton, 1970; 1977) exhibited a similarity between the back-calculated strength at long-term first-time failure and the fully softened strength. The recommended laboratory procedure to measure the fully softened strength was suggested by Skempton (1977) to be the measurement of the strength of remoulded normally consolidated clay. As such, by this definition, the fully softened strength is equivalent to the critical state strength. The results of Skempton's back analyses of first-time failures in cut slopes in London Clay are reproduced here as Fig. 2. As shown in this figure, the strength at failure for each of the five case studies reported by Skempton (1977) plots significantly below the peak strength of the London Clay, well above the residual strength, and is quite consistent with the critical state strength $\phi'_{cs} \approx 20°$. Accordingly, Skempton advised the use of the fully softened strength in association with the highest foreseeable pore water pressures, for design against long-term first-time failure in stiff, fissured clays.

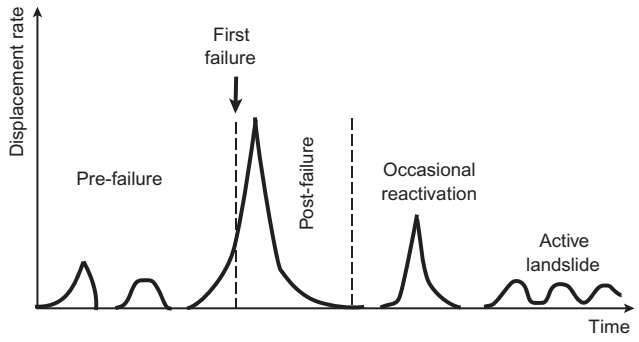

Fig. 1. Stages of slope instability (Leroueil, 2001)

Cooper *et al.* (1998) report the first-time failure of a cut slope in stiff Gault clay which they induced artificially by recharge. A shear rupture was reported to propagate inwards from the toe of the slope, as inferred from inclinometers. Their limit equilibrium analyses showed good agreement with the location and timing of the failure in relation to the observed pore pressures and their estimate of the 'fully softened strength' parameters. They also report that a back-analysis using residual soil strengths in those locations where a shear rupture had been inferred, and peak strength parameters elsewhere, was equally successful. They concluded that the success of Skempton's approach was coincidental but that it was empirically justified as a design method.

Finite-element analyses (FEAs) of a proposed mechanism of progressive failure of cut slopes in stiff clay, through the growth of a residual shear surface, were reported by Potts *et al.* (1997), and suggested as a contributory factor in delayed failure. In these analyses the mechanism of progressive failure has been reproduced by modelling the soil as an elasto-plastic material in which the strain softening of the clay material is accounted for by allowing the strength parameters c' and ϕ' to be a function of the deviatoric plastic strain.

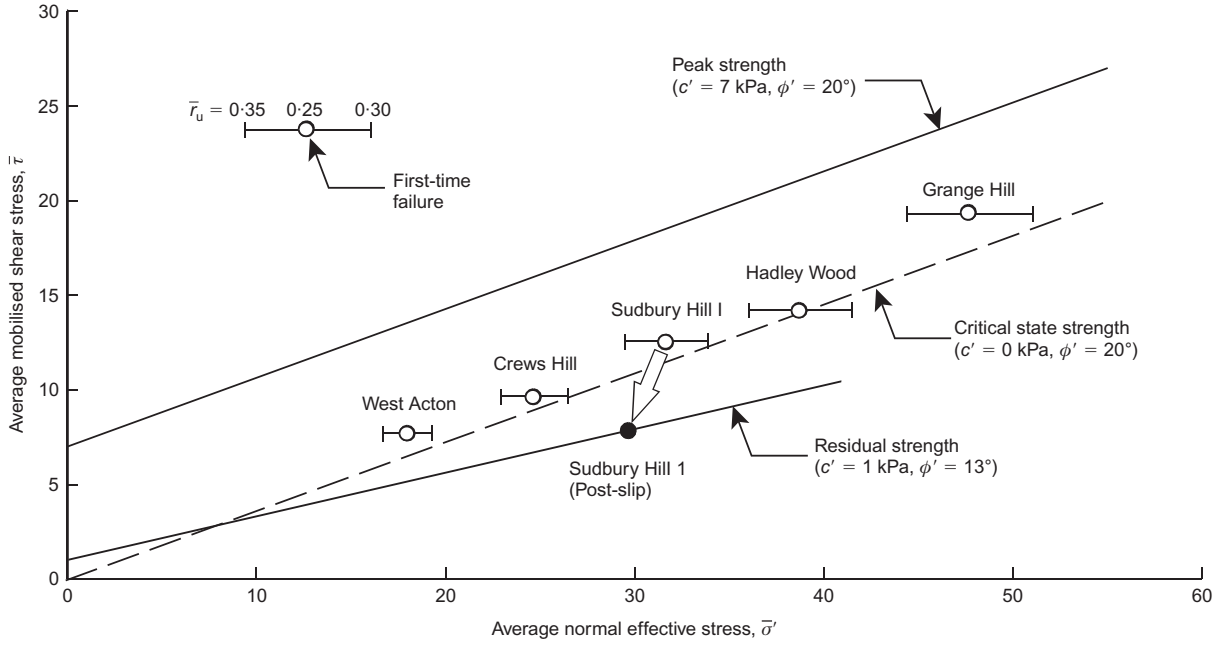

Fig. 2. Strength at first-time failure (Skempton, 1977)

Thus, as plastic strains develop at the toe of the slope over time, the strength in this region is permitted to drop steadily from the peak to the residual, causing stress redistribution to occur and the slope to progress slowly towards first-time failure. Strain-softening of this sort inevitably leads to the growth from the toe of a highly localised residual shear rupture surface.

Leroueil *et al.* (1996) have proposed that the behaviour of slopes prior to first-time failure is influenced by stress changes due to regrading, and by effective stress changes due to varying infiltration, which might lead to progressive failure due to brittleness analogous to fatigue (Leroueil, 2001). Leroueil also suggests that creep, either at constant effective stress or arising from seasonal changes of water content, may induce an additional component of time-dependent softening. With the recent development of high-capacity tensiometers (HCT) by Ridley & Burland (1995), the true magnitude of seasonal stress cycles can now be measured. Such observations have led to the elaboration of the hypothesis that seasonal moisture cycles can drive the mechanism of progressive failure in overconsolidated clay slopes (e.g. Kovacevic *et al.*, 2001; Picarelli *et al.*, 2001; Take & Bolton, 2004). Similarly, recent developments in image analysis techniques for the measurement of soil deformations (e.g. White *et al.*, 2003) have now enabled the measurement of deformations in physical models to a precision and a level of detail previously unattainable. The objective of this paper is to take advantage of these two advances in experimental testing to investigate Skempton's design recommendation with regard to first-time failures through the observation of the underlying mechanism of pre-failure seasonal deformations in a heavily overconsolidated clay, using the technique of geotechnical centrifuge modelling.

EXPERIMENTAL METHODOLOGY

Using the technique of centrifuge testing, the behaviour observed in small-scale soil models can be made representative of field-scale performance (Schofield, 1980). In particular, the accelerated time scale for seepage flow makes this technique particularly well suited to the difficult problem of obtaining coupled stress–deformation data describing the long duration processes that lead to the first-time failure of overconsolidated clay slopes. In the present study, the role of seasonal moisture cycles in progressive failure was assessed by subjecting a model slope both to its own self-weight and to realistic seasonal pore water pressure variations using an atmospheric chamber. Further details of this device are reported by Take & Bolton (2002).

As discussed by Leroueil (2001), the strength parameters determined from the back analysis of actual slope failures are highly sensitive to the assumptions used to calculate them. For most field case studies, the geometry of the slope, the location of the failure surface, the applicability of two-dimensional methods of analysis and the pore water pressure distribution at the time of failure are unknown and must be estimated. In contrast, for the case of a centrifuge model slope, these parameters can be specified or directly observed as follows.

(*a*) Slope geometry and applicability of two-dimensional back analyses: plane-strain analysis of a model slope of height 140 mm (corresponding at 1/60th scale to 8·4 m high) and width 200 mm, with a slope angle of 36°, offering less than 5% error in the inferred soil strength due to the neglect of possible effective friction $\delta = 12°$ acting on the sides of the observed slip zone.

(*b*) Slope material and stress history: Speswhite kaolin clay one-dimensionally consolidated to a maximum vertical effective stress of 500 kPa (unit weight at $1\boldsymbol{g} = 17{\cdot}9$ kN/m^3)

(*c*) Location of the failure surface: deformations can be captured throughout the entire vertical slope cross-section using a digital-image-based deformation measurement system, geoPIV (White *et al.*, 2003), which combines the technologies of digital imaging, close-range photogrammetry and the image-processing technique of particle image velocimetry (PIV).

(*d*) Pore water pressures: eight miniature high-capacity tensiometers (HCTs), saturated under strictly controlled conditions (Take & Bolton, 2003), buried within the model to observe the pore water pressure distribution within the slope (Fig. 3).

OBSERVED SEASONAL SLOPE BEHAVIOUR

Prior to centrifuging, the initial suction in the model was −60 kPa owing to the final unloading increment of the consolidation stage of preparing the clay sample. Using the technique of Take (2003), the self-weight of the model slope was increased in stages of applied centrifugal acceleration, while the atmospheric chamber was set to model a drying season, to encourage negative water pressures to develop in the slope. As a result of this experimental procedure, the slope remained entirely in suction (Fig. 3) during this self-weight loading event. Consequentially, the process of 'gravity turn on' was successfully accomplished without initiating undrained plastic deformations in the slope model.

Once at the testing acceleration of 60$\boldsymbol{g}$, the model was subjected to idealised seasons of alternating wet and dry conditions. According to the principles of centrifuge modelling, model distances are scaled down by a factor n, and the seepage flow velocity is increased by a factor n, so that consolidation times are reduced by n^2, where n is the centrifuge acceleration expressed in gravities. Thus, in a 1/60th scale model subjected to a centripetal acceleration of 60$\boldsymbol{g}$, 2·43 h of seepage flow corresponds to a full calendar year of flow in the field. This time was approximately split in a 5 month/7 month ratio of the lengths of the wet and dry seasons.

The seasonal boundary condition applied to the model surface is recorded as a time history of relative humidity in Fig. 4(a). In this figure, dry seasons can be identified as periods in which the relative humidity of the air above the clay slope is kept constant at approximately 40%, and wet seasons (shaded in grey in the figure) as periods of modelled rainfall created by injecting water into suspended misting nozzles, thereby bringing the air to 100% relative humidity. The pore pressure response to this phase of testing is illustrated in Fig. 4, where time waypoint '0' corresponds to the onset of centrifuge acceleration, and waypoint 'A' identifies the end of a period of pore pressure dissipation after the final self-weight load increment to 60 gravities. In Fig. 4, parts (b) through (e) correspond to pore pressure traces of the top four HCTs that comprise HCT array 1 as defined in Fig. 3. As expected, the seasonal pore water pressure variation is greatest at shallow depths and decreases with increasing depth.

The seasonal pore pressure response to the applied environmental loading is perhaps best observed in the profile of pore water pressures recorded by HCT array 1, shown in Fig. 5. In this measurement array the HCTs were placed along a vertical line within the slope at a spacing of 20 mm. As discussed earlier, the slope had been encouraged to develop a negative pore water pressure profile concurrently with the application of centrifugal acceleration to the slope. This profile is linear and is denoted by time waypoint 'A' in Fig. 5(a). Pore pressure isochrones at intervals of 200 s are

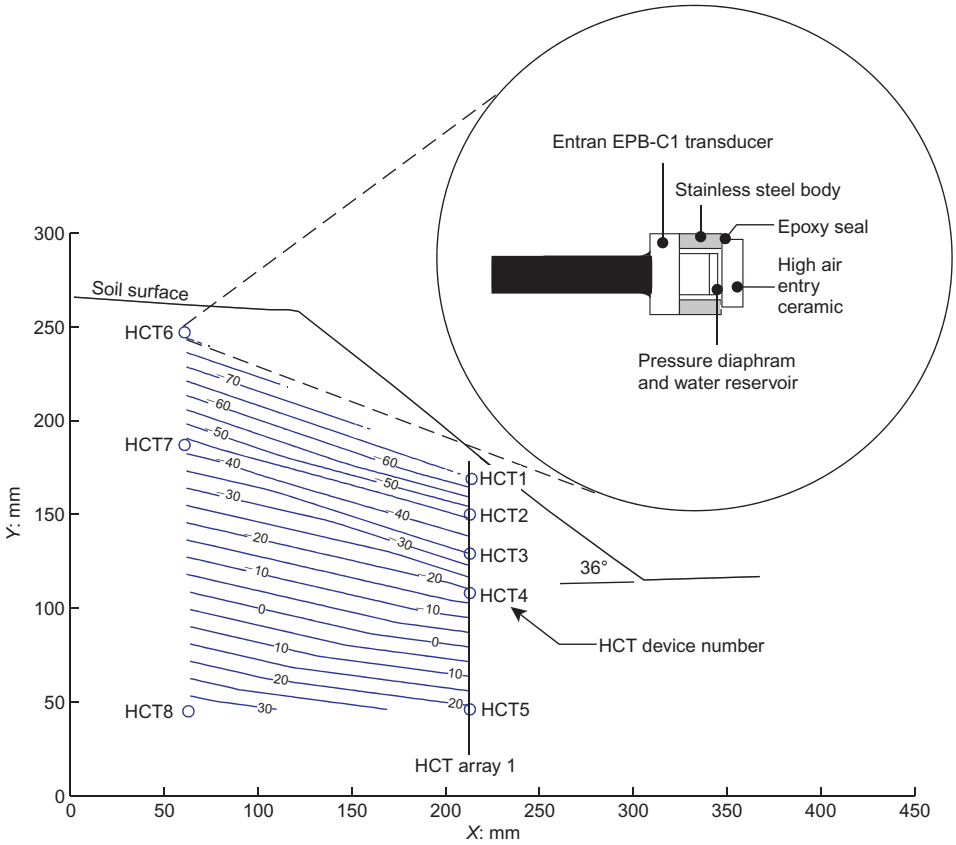

Fig. 3. Measurement arrays of miniature high-capacity tensiometers (HCTs) with contours of interpolated pore water pressures (units: kPa) prior to rainfall infiltration

then presented from this initial state until the end of the first wet season. With the onset of rainfall infiltration, the suctions generated over the long consolidation period are quickly quenched, beginning at the soil surface, but progressing rapidly with depth. As the pore water pressures approach their end-of-season values, the rate of increase slows dramatically as demonstrated by the reduced spacing between the isochrones. Unlike the rapid advance of the pore pressure profile observed under the initial action of rainfall infiltration, the isochrones associated with the first dry season (Fig. 5(b)) exhibit a slow and steady descent into suction. A further contrast with the wet season is the end-of-season pore pressure values. During the wet season, the pore pressure relatively quickly becomes asymptotic to the end-of-season value. In contrast, the maximum value of suction at the end of a drying season (i.e. at the soil's residual moisture content) depends on the duration of the season. The range of suctions imposed on the model surface was specifically chosen to be less than the air entry value of the clay to enable the simplifying assumption of saturated soil behaviour to be made. The seasonal pore water pressure cycle during a typical dry season (Fig. 5(b)) and wet season (Fig. 5(c)) corresponds to a pore water pressure change of approximately 40 kPa at a model depth of 20 mm and approximately 10–15 kPa at a model depth of 80 mm.

The typical seasonal deformation response of the clay slope to these environmental loading cycles is presented as profiles of observed displacements in Fig. 6. Because of a temporary loss of camera connectivity due to a communications error between times B and C, the incremental seasonal deformations will be discussed in relation to the interval D to H. During one such dry season (Fig. 6(a)), the incremental displacement vectors are predominantly normal to the slope and increase in magnitude with elevation in the clay. In contrast, the vectors capturing wet season swelling (Fig. 6(b)) are confined closer to the soil surface and, although inclined predominantly normal to the slope in the crest region, contain increasingly significant down-slope components as the position of the measurement patch approaches the toe of the slope.

Since PIV calculates displacements at any specified location in an image, the measurements can be geometrically organised to form the nodes of virtual strain elements. Using this technique, hundreds of experimental strain elements were defined in the visible plane strain section of the model to enable the shear and volumetric strains to be calculated throughout the model. Here, strains are expressed as total rather than incremental strains to capture the full extent of the damage accumulated with the passage of seasons. For the sake of brevity, only the strain profiles at the ends of the second and fourth wet period are given here as Fig. 7 and Fig. 8. At the end of the second wet season (time waypoint D), the slope has been subjected to a significant amount of shearing, with a strain concentration of 4% total maximum shear strain being observed in the toe region (Fig. 7(a)). Furthermore, the application of the seasonal environmental loading has caused the overconsolidated clay to experience volumetric expansion (denoted by the contours of negative total volumetric strain in Fig. 7(b)). The distribution of volumetric strain contours generally follows the slope profile, which is indicative of swelling. However, it should be noted that an additional concentration of negative volumetric strain is coincident with the zone of shear strain concentration, indicative of dilative shearing in this region. During the next dry season, the contours of shear strain indicate a reversal in the direction of shearing, followed by the accumulation of additional plastic strains in the toe region repeated in the next two wet seasons. This accumulation of

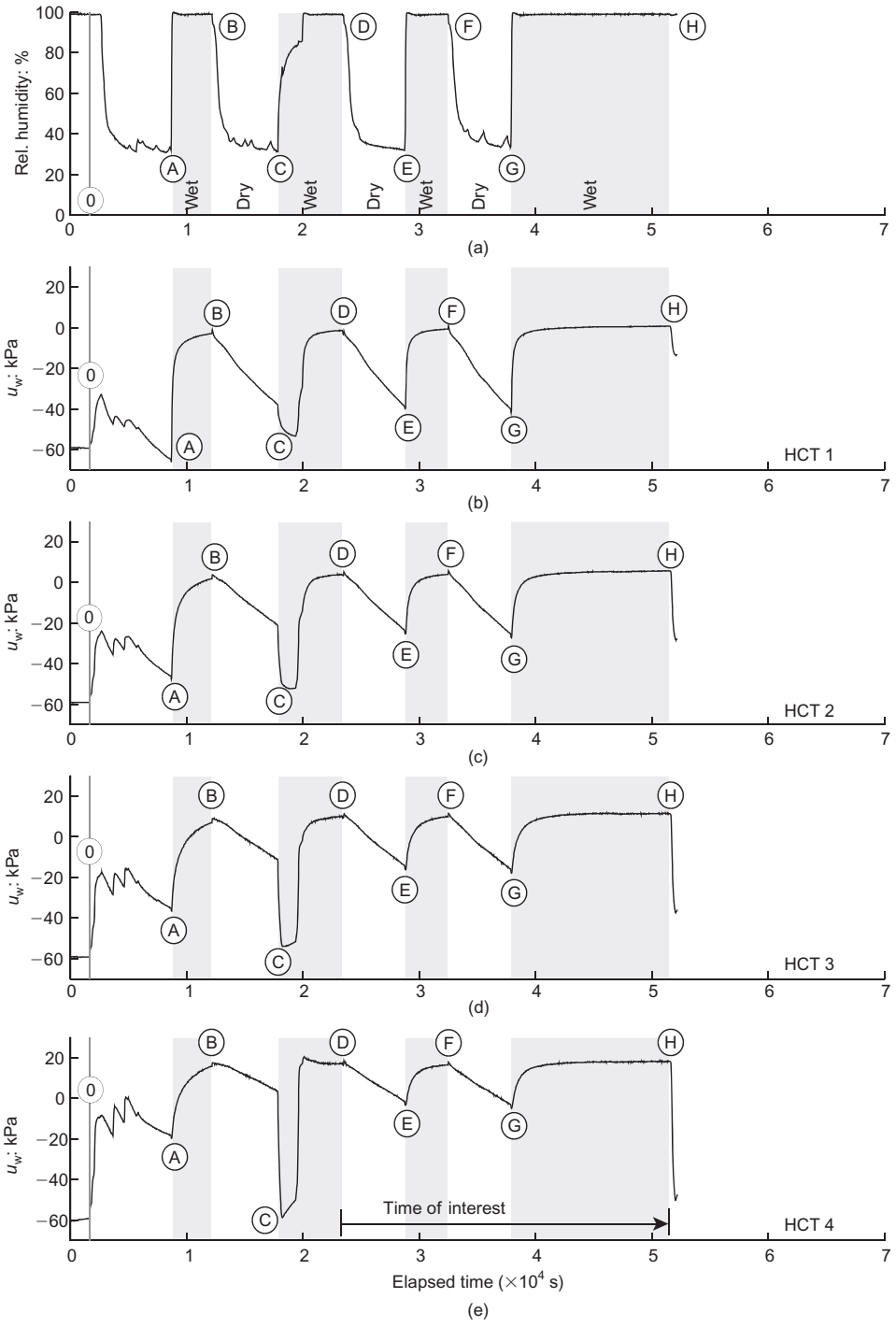

Fig. 4. Applied seasonal boundary conditions

plastic strains led eventually to the onset of progressive failure at the toe (as witnessed by the closely spaced vectors of strain) at the end of the fourth wet season (Fig. 8(a)) and a large region of softening (Fig. 8(b)).

BACK ANALYSIS OF MOBILISED STRENGTH

The coupling of seasonal transient flow with material strain-softening or creep makes the FEA of heavily over-consolidated clay slopes very challenging; such modelling requires a highly advanced constitutive model. Since the aim of the current work is to discover the underlying physical mechanisms of softening, and to offer practical guidance to designers, it was decided to forego FEA in favour of simpler limit equilibrium analyses. At the same time, it was decided to couch the findings of these analyses in terms of the conventional parameters c', ϕ' of the Mohr–Coulomb strength envelope in terms of effective stresses. Thus, as a first attempt, the observations of seasonal slope behaviour in the centrifuge models will be back-analysed using Spencer's method (Spencer, 1967).

An assumption common to all limit equilibrium slope stability methods is that the same proportion of the maximum available shear strength is deemed to be mobilised on the base of each of the vertical slices. This reduction factor is generally expressed as a factor of safety (FOS) for the whole mechanism – a ratio of the available shear strength at failure to the shear stress which must be mobilised for equilibrium. The incompatibility of this assumption with observations that slopes fail in a progressive fashion is

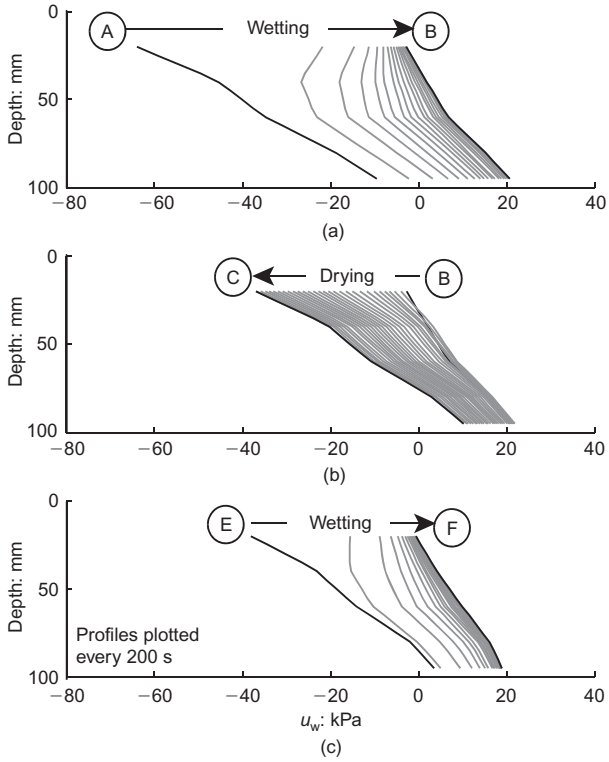

Fig. 5. Seasonal variation of pore water pressures recorded along HCT array 1 during: (a) the first wet season, and subsequent (b) dry and (c) wet seasons

obvious: Fig. 7 and Fig. 8 clearly show a variation of shear strain along all potential failure surfaces leading ultimately to localised failure at the toe. Further, the profiles of volumetric strain in these same figures imply that softening will also be non-uniform. Nevertheless, the classical limit-equilibrium assumption that the degree of mobilisation of soil strength will not depend on the location within the slope, will be adopted here for its simplicity and transparency, while being mindful of its inherent weaknesses.

It is well known that the envelope of peak strength of soils is generally curved and will eventually meet the critical state line at a critical effective stress just sufficient to crush the microstructure and suppress dilatancy (e.g. Cheng *et al.*, 2005; Schofield, 2006), when the overconsolidation ratio (OCR) is about 2·5. As a result the peak strength envelope for a highly overconsolidated clay will be curved at the low confining stresses typical of shallow slope failures (Fig. 9(a)). As has been discussed by Atkinson (2007), a linear Mohr–Coulomb failure criterion applied to peak strength data is intrinsically unsafe when the normal effective stresses in the ground are either higher or lower than the effective stresses applied in the shear tests. An example of this is included as Fig. 9(a), which illustrates the ease with which the peak strength can be overestimated using a linear curve fitted to two tests performed at high effective confining stresses. The curved peak strength envelope, therefore, requires careful attention to stress level if a linear envelope is used in limit equilibrium slope stability analyses.

Rather than back-calculate the evolution of the slope's FOS with time, an alternative strategy has been adopted in which the FOS is set at 1·0 and the strength parameters required to be mobilised along the length of the failure surface are back-calculated at frequent intervals of time. In order to perform this back-analysis, a rule for invoking the two strength parameters, c'_{mob}, and ϕ'_{mob} must be defined. Otherwise, there are infinite numbers of combinations of these two mobilised strength parameters that could be used to define the average stress ratio along the critical slip surface. The rule used in the present study is presented in Fig. 9(b). Here, an arbitrary stress point defining the average shear and normal stress acting along the length of a failure surface can be defined using the parameters c'_{mob} and ϕ'_{mob}. If the stress point lies to the right of the critical state stress ratio, such as stress point '1', the average stress point can be described by an average mobilised frictional strength component, ϕ'_{mob}, and a zero cohesive strength component. As pore pressures rise, during rainfall infiltration, the stress point will move to the left, which is indicated in the analysis as an increase in the current mobilised friction. As shown by stress points '2' and '3' in Fig. 9(b), the frictional component of strength is capped at the critical state angle, in this case $\phi'_{\text{cs}} = 24°$ for Speswhite kaolin clay (based on an average of values reported in the literature, including Clegg (1981) and Atkinson (2007)). An additional rise in pore pressures will therefore cause the average stress ratio in the slope to increase, represented by the capped frictional resistance at the critical state angle and the introduction of a component of mobilised true cohesion, c'_{mob}.

Defining the mobilised peak strength envelope as parallel to the critical state line is, strictly speaking, incorrect. The mobilised shear resistance of slices with very high or low normal effective stresses will be overestimated (Fig. 9(b)). However, the objective of the current analysis is to understand the mobilisation of soil strength well *below* its peak value. The magnitude of the error associated with this simplification obviously depends on the OCR of the points under consideration on the trial slip surface (i.e. the position of the mobilised strength line within the peak strength envelope of Fig. 9(b)). If the OCR is high, as is the case in the present study, the magnitude of the error will be small. The obvious virtues of this c'_{mob} assumption are simplicity and transparency. It is, in any event, the simplification adopted by most authors in dealing with the difference between peak strength and critical state strength envelopes of clay slopes, following Skempton (1977).

The aim of the modified Spencer analysis is to estimate the average stress path followed by the model slope as time progresses and the seasons pass. However, the position of the critical failure surface will rise and fall within the slope with the passage of seasons. Rather than account for this additional complication, the strength mobilised in the model test will be calculated only for the critical slip circle found for worst-case conditions – in this case, at the end of the longest wet season, wet season 4 (H). The results of this analysis are presented in Fig. 10. Using an iterative solution, the effective shear strength parameters (c'_{mob}, ϕ'_{mob}) just necessary to maintain equilibrium at that instant have been back-calculated. The resulting failure surface is relatively shallow (within the top 3 m at prototype scale) and indicates that the model slope at waypoint H must have been mobilising, on average, a peak strength of $c'_{\text{mob}} = 7{\cdot}5$ kPa and $\phi'_{\text{mob}} = 24°$.

Limit equilibrium design calculations for slope stability are usually undertaken assuming the worst credible scenario for pore water pressures. However, in the present study, the observations of seasonal pore water pressures can be used to calculate the varying seasonal mobilisation of strength on the ultimate critical failure surface. The results from these back analyses are presented in Fig. 11 in terms of c'_{mob} and ϕ'_{mob}. These data indicate that initially, at time waypoint A, the magnitude and distribution of negative pore pressures through the slope profile require only a mobilised frictional strength of 12° to maintain equilibrium. As wet seasons are induced, the effective stress ratio which must be mobilised within the kaolin increases, leading to episodic periods in

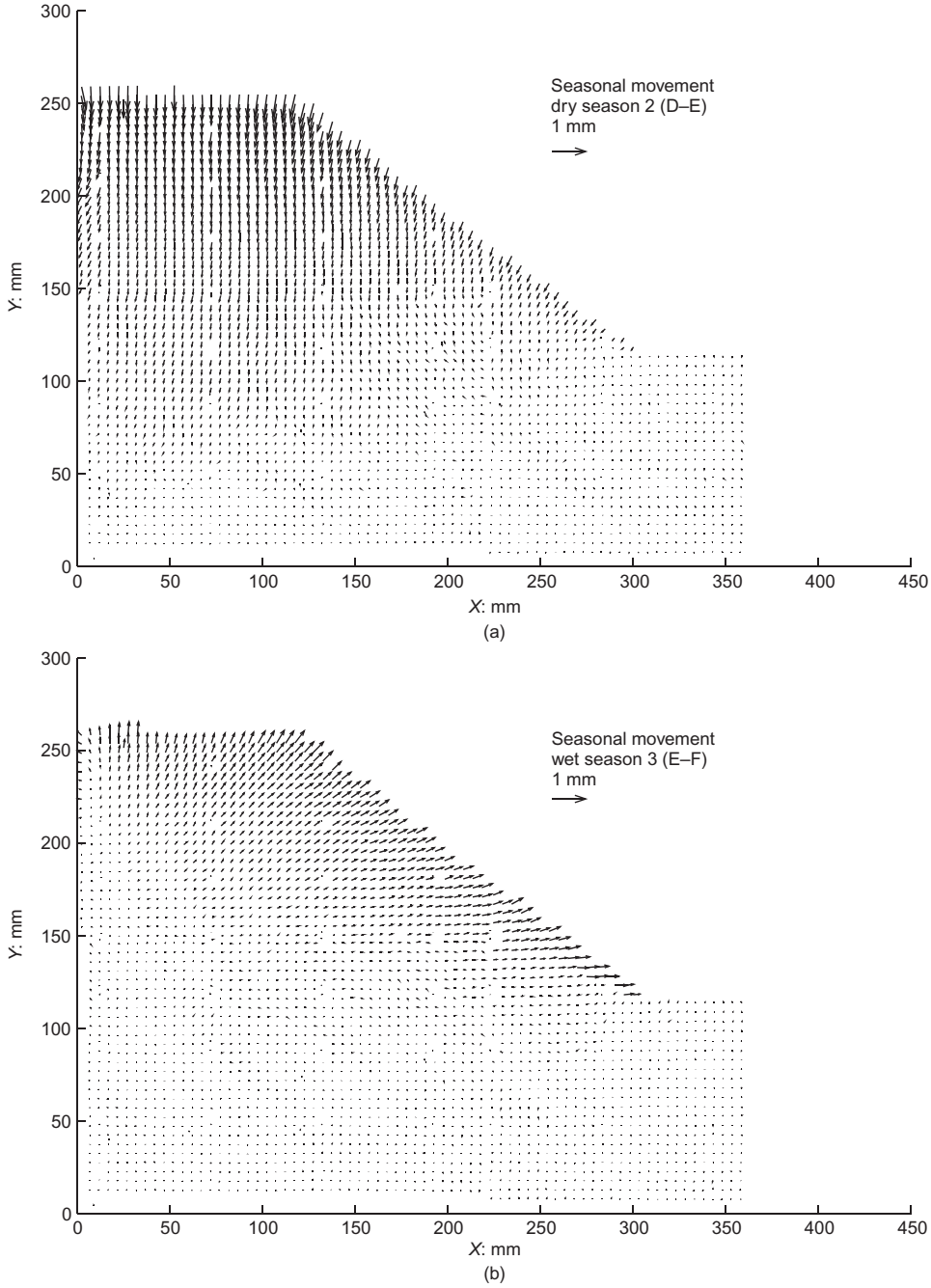

Fig. 6. Typical measured vectors of seasonal shrinkage and swelling

which some portion of peak strength (c'_{mob}) is required to be mobilised to maintain stability.

CORRELATING STRENGTH AND DEFORMATION MEASUREMENTS

The environmental loading of seasonal moisture cycles has been shown to produce significant irrecoverable regional softening below a slope in clay. The limit equilibrium method described in the previous section allows an estimation of the average stress path travelled by soil elements lying on the slope's critical failure surface. The results from these analyses indicate that the soil slope relied successfully upon the temporary mobilisation of super-critical stress ratios for short-term stability. There remains the question of whether the mobilisation of super-critical stress ratios will affect long-term stability. This question will be investigated by combining the back-calculated mobilised strength and the observed PIV deformation data to provide correlated stress and deformation measurements throughout the cross-section of the model.

The evaluation of seasonal deformations will be made for 36 PIV patches of soil, each lying 3 mm below the soil surface at the end of the second dry season of the analysed test. These patches are spaced at 10 mm centres, and cover the entire slope surface from the side of the centrifuge container (which might be regarded as the plane of symmetry through the centre of a prototype embankment) to the toe of the slope. As shown in Fig. 12(a), every second patch is named with a lower case letter to enable further discussion in this section. In this figure, vectors of total displacements are presented from the patch's initial position at the end of the second dry season to the patch's final position at the end of the fourth wet season. Although these incremental displacement vectors describe the general behaviour of vertical displacements within the crest and shear displacements

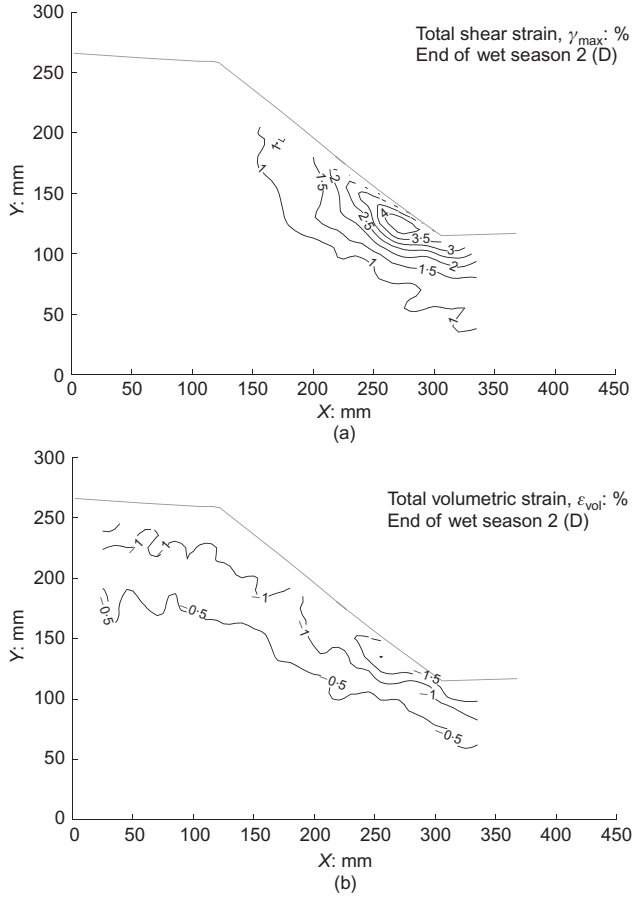

Fig. 7. Measured total strain at the end of wet season 2 (time waypoint D)

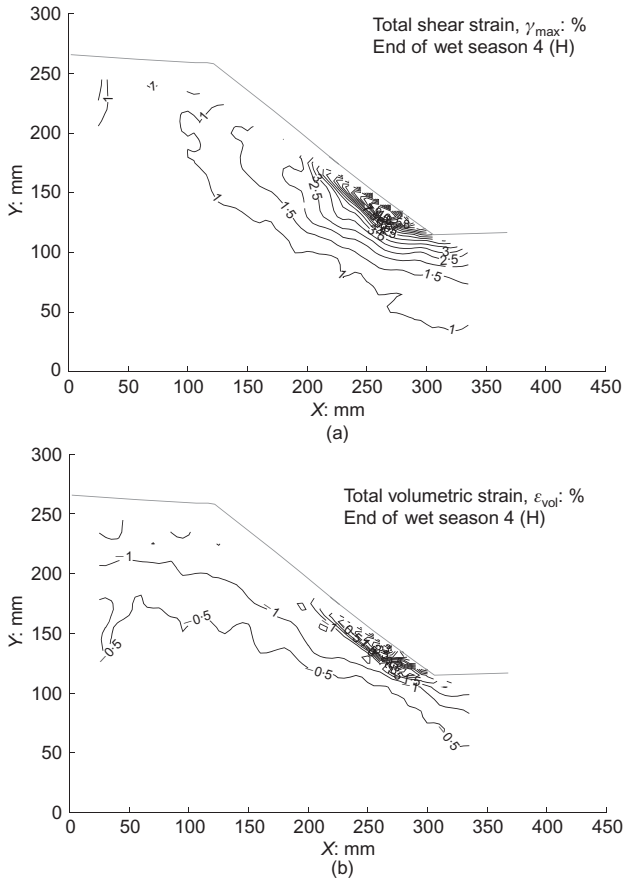

Fig. 8. Measured total strain at the end of wet season 4 (time waypoint H)

at the toe over this time period, much of the detailed seasonal behaviour is lost unless the entire series of 351 digital images taken over this time period is considered. This detailed behaviour is documented for a patch near the mid-height of the slope, patch 'j' in Fig. 12(b). At test waypoint D, the patch is considered to be at the origin of the plot of relative displacement. Each subsequent dot on the figure is an observation of the position of the soil element relative to this baseline position. Thus, as the dry season begins, the soil element is observed to retreat under the action of shrinkage and travel in a direction predominantly normal to the slope surface. The onset of the wet season reverses this trend at test waypoint E, and the soil patch initially retraces the shrinkage path before travelling in an increasingly lateral direction. This lateral movement is interrupted by the arrival of the dry season, when the down-slope displacement reduces, and the patch shrinks in a direction approximately normal to the soil slope. The fourth wet season arrests the shrinkage at test waypoint G, and causes the soil to swell in a direction retracing the shrinkage path before travelling in an increasingly lateral direction. For an element of soil in the middle of the slope, this results in a displacement path with at shape similar to the letter W, demonstrating an irrecoverable down-slope ratcheting of the slope surface under the action of the environmental loading.

The behaviour in the other regions of the slope can similarly be tracked with time. The seasonal deformation paths of the 16 patches, identified as patches 'a'–'p' in Fig. 12(a), are presented in Figs 13(a)–13(p), respectively. On the crest of the model slope (patch 'a'), the soil is shrinking and swelling entirely vertically. Towards the shoulder, there begins to exist a component of lateral movement during the wet season. Further along the line of patches, the horizontal movements increase while the vertical movements decrease. Finally, at the toe of the slope (patch 'o'), the soil element is moving almost entirely in the horizontal direction. Yet, 10 mm into the clay from the toe of the slope (patch 'p'), the soil is essentially motionless.

The observed displacements at these locations can be correlated with the average back-calculated mobilised strength by plotting these data along their shared time axis. In order to highlight the irrecoverable components of slope movements, the displacement will be presented in a local coordinate system corresponding to the direction of local swelling. An example of the chosen coordinate system is defined in Fig. 12, for PIV patch 'j'. Here, the direction of swelling has been chosen by performing linear regression on the data points describing the initial linear swelling displacement at each PIV patch location. Displacements normal to the direction of swelling correspond to mostly irrecoverable seasonal shear deformations. These local coordinates may therefore be treated approximately as though they were the vertical and horizontal displacements of the loading platen of a direct simple shear test on a sample taken so that the horizontal shear direction in the laboratory would correspond to the local inclination of shearing in the field.

The correlated stress–displacement data for the PIV patches 'a', 'j' and 'o', corresponding to the top centre, middle and toe of the model slope, are presented in Fig. 14. The observed displacement of patch 'a' located at the top of the slope is effectively one dimensional. The seasonal displacement of this patch is entirely vertical with settlement in the dry seasons DE and FG exceeding swelling in the wet seasons EF and GH. Superimposed on Fig. 14 are the periods of time in which the slope mobilises super-critical strength; however, no correspondence can be identified for

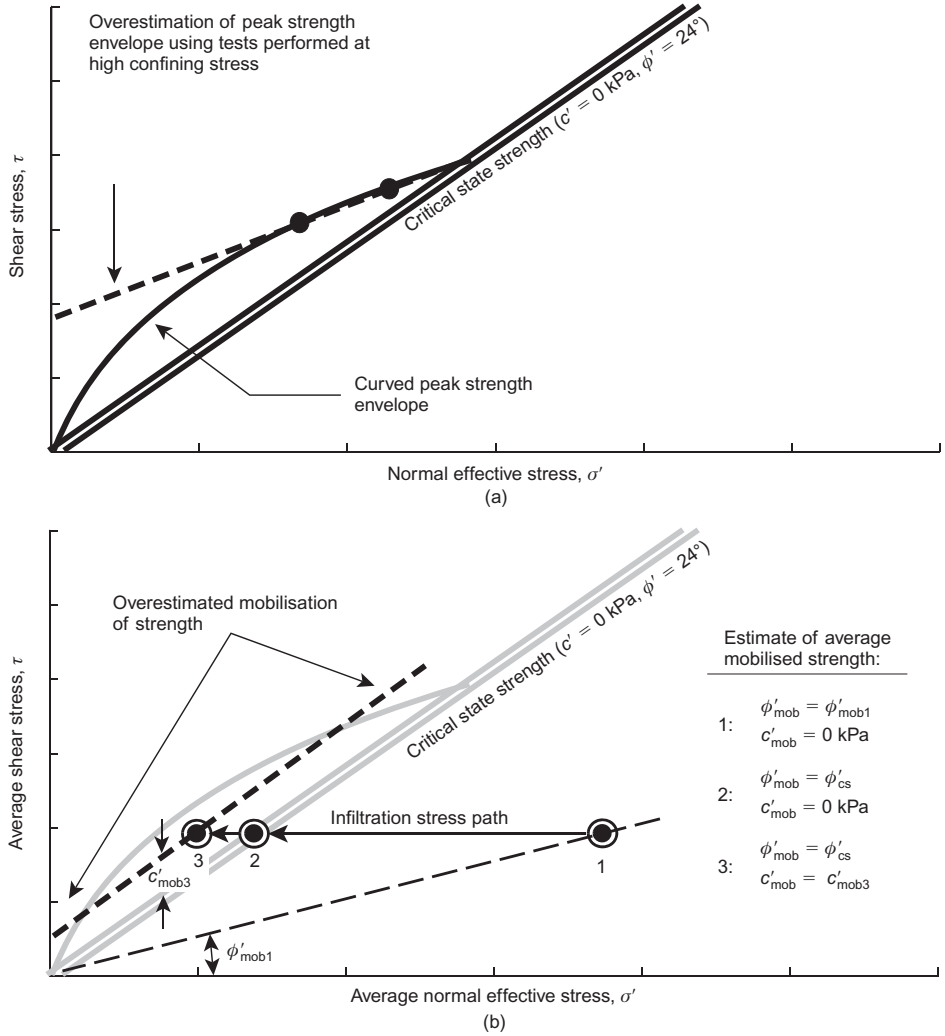

Fig. 9. (a) Schematic diagram of a curved peak strength envelope for overconsolidated clay. (b) An estimation methodology for calculating average mobilised strength in terms of c'_{mob} and ϕ'_{mob}

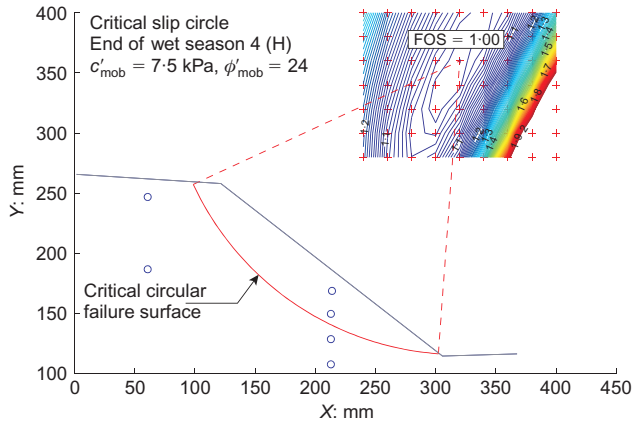

Fig. 10. Estimation of average mobilised strength at the end of the most severe wet season (time H)

patch 'a'. At the mid elevation of the slope, PIV patch 'j', the slope is also experiencing displacement in the direction of swelling, but the dry season shrinkage DE and FG roughly balances the wet season swelling EF. There is also a significant component of displacement normal to the direction of swelling (Fig. 14(b)) which increases monotonically but episodically, with each occurrence corresponding to the period of time over which super-critical strengths are mobilised on average throughout the slope. At the toe of the slope, the wet season heave EF far exceeds the dry season settlements DE and FG. The shear displacements normal to the direction of swelling correspond approximately to the period in which the critical slip mechanism requires the slope to mobilise increasing super-critical strength, and they are almost completely irrecoverable. Ultimately, the degree of softening at the toe together with the high pore pressures developed during the final, long wet season were sufficient to provoke the detachment of a soil segment. Fig. 15 shows that this portion of toe of the slope experienced shear rupture along its base until truncated by the rapid formation of a tension crack at its upper edge.

These displacement histories correspond approximately with the behaviour that would have been expected in direct simple shear tests on dilatant soil, in which normal effective stress varies while the shear stress remains constant. Elastic swelling and recompression accompanied excursions of pore pressure at sub-critical effective stress ratios. Plastic shear strains inducing dilation and softening accompanied the mobilisation of super-critical stress ratios. Accordingly, the transitions from elastic to plastic behaviour of the representative soil patch 'j' during wet seasons EF and GH are seen in Fig. 12(b) to coincide approximately with the points

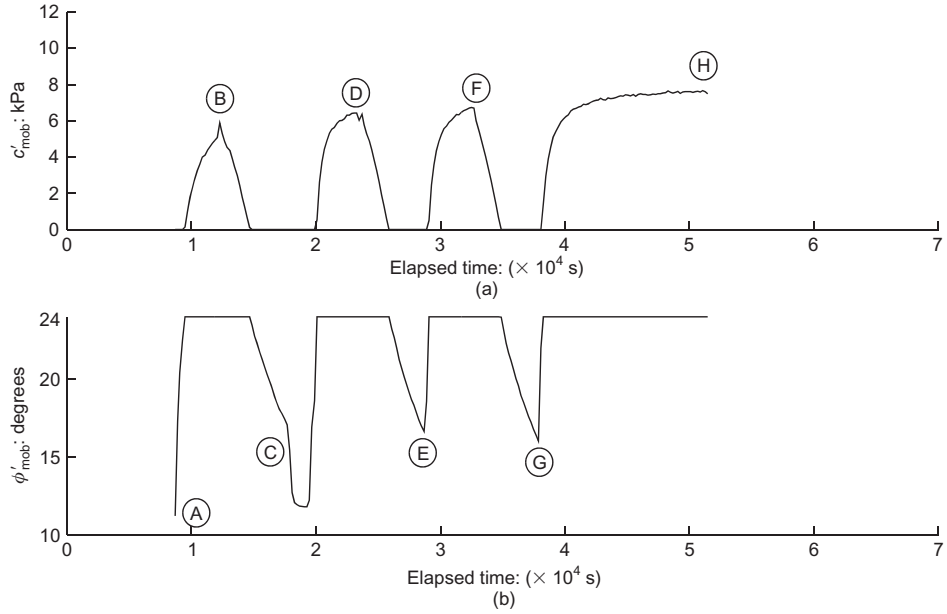

Fig. 11. Seasonal mobilisation of soil strength, Spencer's method

marked CSR at which the average strength mobilisation passes the critical state stress ratio, therefore just satisfying the condition $c'_{mob} > 0$. The final separation of the toe segment, however, could not easily have been reproduced in any conventional element test, since it apparently relied on the opening of a tension crack to the free surface of the slope.

DISCUSSION

Despite the limitations and assumptions of the modified Spencer back-analysis, the results acquired using this technique have demonstrated clearly, in Fig. 14(a), that any temporary mobilisation of super-critical stress ratios by a slope will be accompanied by plastic deformations. This observation is entirely consistent with a view of soil mechanics embodied by Taylor's work equation (Taylor, 1948), reproduced below in equation (1) in terms of friction angles

$$\tan \varphi'_{mob} = \tan \varphi'_{cs} + \frac{\delta \varepsilon_v^p}{\delta \gamma^p} \quad (1)$$

where, $-\delta \varepsilon_v^p / \delta \gamma^p$ is the rate of plastic dilation, as defined by the ratio of the plastic volumetric strain increment to the plastic shear strain increment. Any process that results in the creation of a plastic shear strain increment $\delta \gamma^p$ should, according to equation (1), produce a corresponding plastic volume change $\delta \varepsilon^p$ which will be positive or negative depending on whether ϕ'_{mob} is smaller or larger than ϕ'_{cs}, respectively. The present authors' work shows that seasonal wetting and drying is one such agent that promotes plastic shearing, and which therefore promotes the dilatant softening of slopes that were mobilising super-critical stress ratios. Conversely, a clay slope which solely mobilises sub-critical frictional resistance should experience neither seasonal ratcheting, nor delayed first-time failure; in that case, seasonal wetting and drying should cause compaction and hardening.

This model of regional softening due to dilatant ratcheting offers a rational explanation for the observation of Crabb & Atkinson (1991) that first-time shallow failures (less than 2 m) of cut or fill slopes in plastic clays can best be back-analysed with the soil's critical state friction angle. The centrifuge test results reported and analysed here have demonstrated regional softening that precedes localisation on a shear rupture in long-term slope failures subject to seasonal wetting and drying. Widespread dilation and softening was observed, increasing season by season so that the original peak strength of the soil becomes increasingly irrelevant to the ultimate failure. Although there was more softening in the region just inside the toe of the slope than at higher elevations, that softening was diffuse. It only led to a localisation failure at the toe after slope movements had already reached about 1 mm (60 mm at prototype scale), creating shear strains of up to 5%. Such movements must probably be considered unserviceable as well as being predictive of a future slip failure, but they can be suppressed by designing to ϕ'_{cs} and by foreseeing worst-case pore pressures as Skempton recommended.

CONCLUSIONS

Highly instrumented centrifuge models of overconsolidated kaolin clay slopes have been subjected to seasonal moisture changes imposed by applied rainfall and relative humidity cycles. The resulting seasonal pore pressures and deformations have been observed using the new technologies of PIV and buried miniature high-capacity tensiometers. Widespread dilation and softening was observed to accompany seasonal downslope ratcheting, leading ultimately to delayed local failure at the toe of the slope. These model tests demonstrate that designs which aim to avoid the long-term failure of clay slopes must take into account the seasonal mechanism of dilatant ratcheting and regional softening

A Spencer limit-equilibrium back-analysis was used with these experimental data to link seasonal moisture cycles and corresponding cyclic effective stress paths within a clay slope to the accumulation of plastic strains, and to the onset of a first-time long-term failure. This rather straightforward limit-equilibrium approach was sufficient to illustrate that the initial pre-rupture phase of regional softening and slope ratcheting was due to the repeated mobilisation of dilatancy in successive wet seasons. If super-critical stress ratios are mobilised, some dilation – irrecoverable softening – must occur. If this happens repeatedly, the softening will eventually be sufficient to cause failure under conditions rather

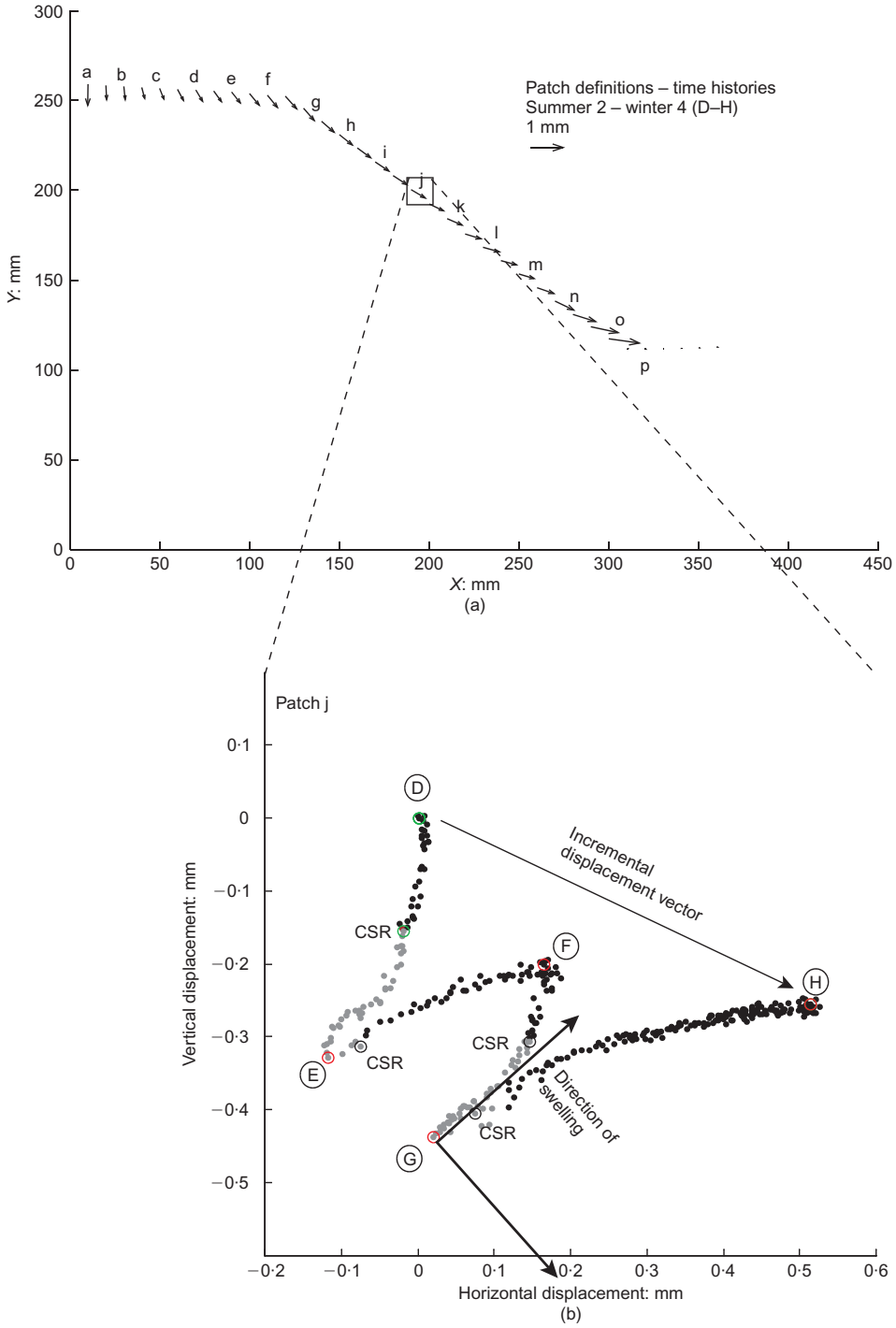

Fig. 12. (a) Observed total and (b) incremental seasonal displacements

less onerous than would have been expected from an analysis using initial peak strengths. From this perspective, the use of Skempton's 'fully softened' strengths has been shown to be appropriate in the design of clay slopes that will be subject to seasonal variations of groundwater conditions.

The designer of any slope in clay should also be aware of the mechanism of progressive failure. The limit equilibrium method invokes unique strength parameters along each potential failure surface. Strictly speaking, this is incorrect. In a slope that mobilises the critical state stress ratio on average, there will be some regions of the slope (e.g. near the toe) that will slightly exceed the critical state stress ratio. If this results in local seasonal irrecoverable dilation, it is possible that the slope might experience progressive failure, albeit at a much slower rate than slopes that uniformly mobilise higher stress ratios. In slopes designed to flout Skempton's advice (such as the model slope described in this paper), seasonal softening will lead to the formation of a rupture, which may well suffer sufficient shear displacement for the soil strength to fall even further to a residual value at first-time failure. However, as far as the authors are aware, no first-time failure has ever been reported of a clay slope designed on simple limit-equilibrium principles using the soil's critical state angle of friction together with worst-case pore water pressures.

This paper has focused on the role of cyclic changes in effective stress ratio leading to seasonal slope deformations, often referred to as 'ratcheting creep', in slopes that repeat-

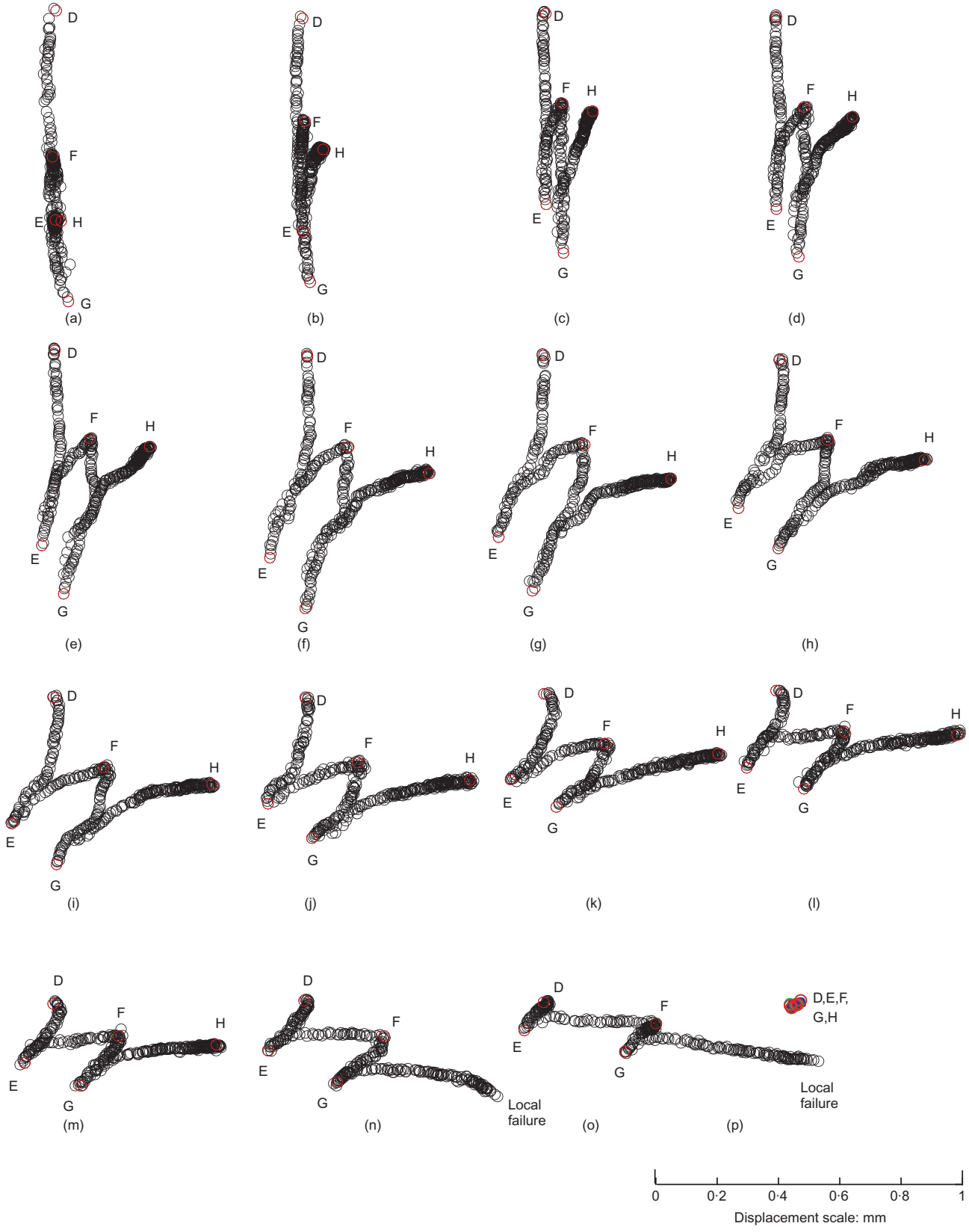

Fig. 13. Seasonal slope deformations at PIV patch locations 'a'–'p'

edly mobilise super-critical stress ratios. Thermally activated creep also occurs without any change in effective stress, but it has not been the focus of the analysis described here. The current study has focused on regional dilatant softening which, acting alone, has been shown to be sufficient to bring a stiff clay slope to failure.

ACKNOWLEDGEMENTS

The authors gratefully acknowledge the funding provided by EPSRC award GR/R91830/01, the Commonwealth Scholarships Commission and the collaboration of the UK Highways Agency and the Hong Kong Geotechnical Engineering Office.

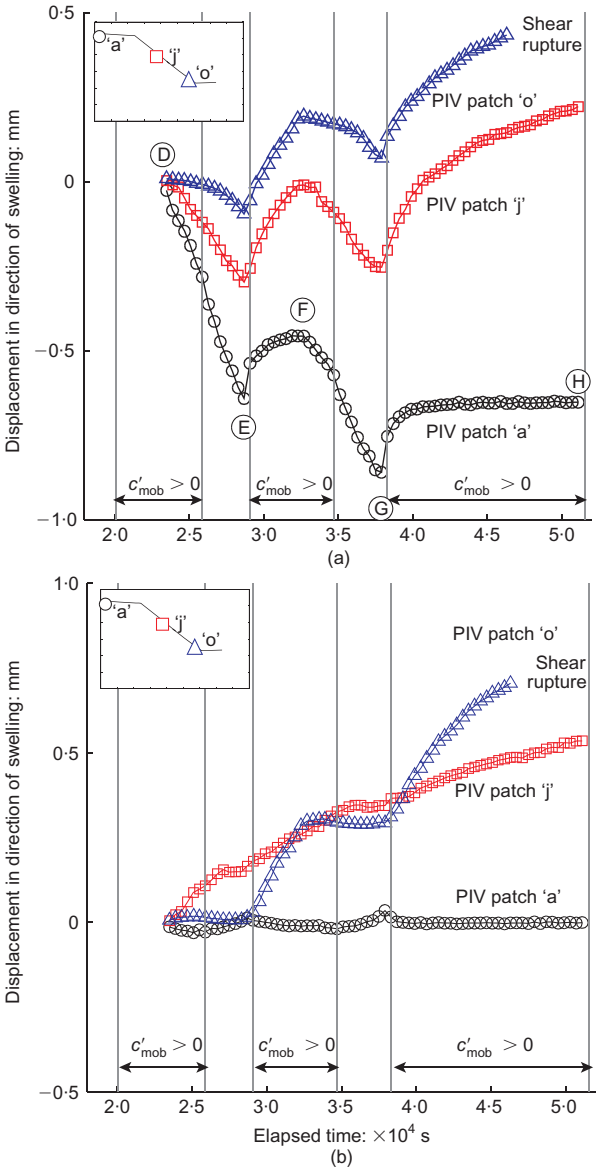

Fig. 14. Seasonal rates of deformation at crest, mid-slope and toe of embankment: (a) in the direction of swelling; (b) normal to the direction of swelling

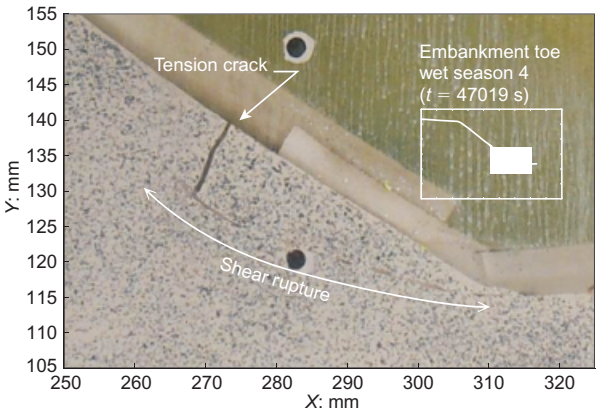

Fig. 15. Shear localisation observed at the toe of the slope at the end of the fourth wet season

REFERENCES

Atkinson, J. H. (2007). Peak strength of overconsolidated clays. *Géotechnique* **57**, No. 2, 127–135, **doi**: 10.1680/geot.2007.57.2.127.

Bishop, A.W. (1967). Progressive failure – with special reference to the mechanism causing it. *Proc. Geotech. Conf., Oslo* **2**, 142–150.

Cheng, Y. P., Bolton, M. D. & Nakata, Y. (2005). Grain crushing and critical state observed in DEM simulations. *Powders and Grains* **2**, 1393–1397.

Clegg, D. P. (1981). *Model piles in stiff clay.* PhD thesis, University of Cambridge.

Cooper, M. R., Bromhead, E. N., Petley, D. J. & Grant, D. I. (1998). The Selborne cutting stability experiment. *Géotechnique* **48**, No. 1, 83–101, **doi**: 10.1680/geot.1998.48.1.83.

Crabb, G. I. & Atkinson, J. H. (1991). Determination of soil strength parameters for the analysis of highway slope failures. In *Slope stability engineering: developments and applications* (ed. R. J. Chandler), pp. 13–18. London: Thomas Telford.

Kovacevic, N., Potts, D. M. & Vaughan, P. R. (2001). Progressive failure in clay embankments due to seasonal climate changes. *Proc. 15th Int. Conf. Soil Mech. Geotech. Engng, Istanbul, Turkey* **3**, 2127–2130.

Leroueil, S. (2001). 39th Rankine Lecture: Natural slopes and cuts: movement and failure mechanisms. *Géotechnique* **51**, No. 3, 197–243, **doi**: 10.1680/geot.2001.51.3.197.

Leroueil, S., Vaunat, J., Picarelli, L., *et al.* (1996). A geotechnical characterization of slope movements. *Proc. 7th Int. Symp. on Landslides, Trondheim* **1**, 53–74.

Picarelli, G., Urciuoli, G. & Russo, C. (2001). Mechanics of slope deformation and failure in stiff clays and clay shales as a consequence of pore pressure fluctuation. Keynote lecture. *Proc. 8th Int. Symp. on Landslides* **2**, 1–34.

Potts, D. M., Kovacevic, N. & Vaughan, P. R. (1997). Delayed collapse of cut slopes in stiff clay. *Géotechnique* **47**, No. 5, 953–982, **doi**: 10.1680/geot.1997.47.5.953.

Ridley, A. M. & Burland, J. B. (1995). A pore pressure probe for the in situ measurement of soil suction. *Proceedings of the conference on advances in site investigation practice*, Institution of Civil Engineers, London, pp. 510–520.

Schofield, A. N. (1980). 20th Rankine Lecture: Cambridge geotechnical centrifuge operations. *Géotechnique* **30**, No. 3, 227–268, **doi**: 10.1680/geot.1980.30.3.227.

Schofield, A. N. (2006). Interlocking, and peak and design strengths. *Géotechnique* **56**, No. 5, 357–358, **doi**: 10.1680/geot.2006.56.5.357.

Skempton, A. W. (1964). Long-term stability of clay slopes. *Géotechnique* **14**, No. 2, 77–102, **doi**: 10.1680/geot.1964.14.2.77.

Skempton, A. W. (1970). First-time slides in over-consolidated clays. *Géotechnique* **20**, No. 3, 320–324, **doi**: 10.1680/geot.1970.20.3.320.

Skempton, A. W. (1977). Slope stability of cuttings in brown London Clay. *Proc. 9th Int. Conf. Soil Mech. Found. Engng, Tokyo* **3**, 261–270.

Spencer, E. (1967). A method of analysis of the stability of embankments assuming parallel inter-slice forces. *Géotechnique* **17**, No. 1, 11–26, **doi**: 10.1680/geot.1967.17.1.11.

Take, W. A. (2003). *The influence of seasonal moisture cycles on clay slopes*. PhD thesis, University of Cambridge.

Take, W. A. & Bolton, M. D. (2002). An atmospheric chamber for the investigation of the effect of seasonal moisture changes on clay slopes. *Proc. Int. Conf. Phys. Modelling Geotech., St John's*, 765–770. Rotterdam: Balkema.

Take, W. A. & Bolton, M. D. (2003). Tensiometer saturation and the reliable measurement of matric suction. *Géotechnique* **53**, No. 2, 159–172, **doi**: 10.1680/geot.2003.53.2.159.

Take, W. A. & Bolton, M. D. (2004). Identification of seasonal slope behaviour mechanisms from centrifuge case studies. *Proc. Skempton Memorial Conf.* **2**, 992–1004.

Taylor, D. W. (1948). *Fundamentals of soil mechanics*. New York: Wiley.

White, D. J., Take, W. A. & Bolton, M. D. (2003). Soil deformation measurement using particle image velocimetry (PIV) and photogrammetry. *Géotechnique* **53**, No. 7, 619–631, **doi**: 10.1680/geot.2003.53.7.619.

Vaughan, P. R. & Walbancke, H. J. (1973). Pore pressure changes and the delayed failure of cutting slopes in over-consolidated clay. *Géotechnique* **23**, No. 4, 531–539, **doi**: 10.1680/geot.1973.23.4.531.